
**13th World Conference on Earthquake Engineering**
**Vancouver, B.C., Canada**
**August 1-6, 2004**
**Paper No. 2130**

# RESPONSE ASSESSMENT OF MEXICAN CONFINED MASONRY STRUCTURES THROUGH SHAKING TABLE TESTS

**Sergio M. Alcocer[1], Juan Guillermo Arias[2], Alejandro Vázquez[2]**

## SUMMARY

The dynamic behavior of two small-scale confined masonry buildings tested in shaking table is discussed. Specimens were half-scale models of typical low-cost housing buildings of one and three stories constructed in Mexico. Models were subjected to a series of seismic motions characteristic of Mexican subduction events recorded in the epicentral region. From recorded and observed results, resistant mechanisms were identified; the structural capacity was assessed in terms of strength, stiffness, deformation and energy dissipation.

## INTRODUCTION

Confined masonry is the most common material used for dwelling construction in Mexico and in many Latin American countries. Low-cost housing projects are constructed using traditional methods for confined masonry. Confined masonry, CM, consists of load-bearing walls surrounded by small cast-in-place reinforced concrete columns and beams, hereafter referred to as tie-columns, TC´s, and bond-beams, BB's, respectively. The system is such that walls must resist both the vertical and lateral loads.

The seismic behavior of confined masonry buildings has been generally satisfactory, particularly in Mexico City. Nevertheless, significant damages have been observed in near-epicentral regions during strong ground shaking. In response to this, new building code requirements have become more stringent thus requiring designs to be revised, and in most cases, be modified substantially to comply with the new ordinances. Since construction programs for multi-family low-cost housing in Mexico involve prototype designs which are repeated several times, the impact on construction cost is very large.

[1] Institute of Engineering, National University of Mexico, Apartado Postal 70-472, Mexico, DF, 04510. Tel: (+52 55) 5622-8946, Fax: (+52 55) 5616-2894, Email: salcocerm@iingen.unam.mx

[2] Institute of Engineering, National University of Mexico, Apartado Postal 70-472, Mexico, DF, 04510. Tel: (+52 55) 5622-8946, Fax: (+52 55) 5616-2894, Email: jara@pumas.iingen.unam.mx

In the past decade, a comprehensive research program of quasi-static tests of isolated masonry walls and systems of walls to natural scale and of nonlinear analyses that contributed valuable information on the behavior to lateral and vertical loads of this type of constructions was carried out in Mexico [1-5]. Nevertheless, little information is still available on the response of three-dimensional confined masonry structures subjected to controlled dynamic excitations, like those applied through shaking tables. Moreover, the wealth of information available is insufficient to compare the expected behavior, based on static tests, to the real response under real events.

To obtain more evidence on the dynamic response of confined masonry, a series of tests are currently underway at the shaking table facility of the Institute of Engineering at UNAM. Due to the large inventory of existing construction in the region, results of this investigation will help in clarifying our understanding of this type of structures, particularly regarding the actual safety factor of real structures. The research program involves construction and testing of one-, two-, three- and five-story small-scale specimens in which wall dimensions, layout and detailing are comparable to typical prototypes. All structures, except the five-story specimen, are built to half scale. The scale for the five-story structure is 2.4. A similitude model for ultimate strength was selected as the basis for scaling. This paper reports on the response of the one and three-story models, hereafter referred to as M1 and M3 specimens.

## EXPERIMENTAL PROGRAM

### Description of the specimens

The shaking table system at UNAM is capable of controlling five degrees of freedom and operating in frequencies ranging from 0,1 to 50 Hz. Due to the physical characteristics of the table (size is 4,0 x 4,0 m, and the maximum weigh of the specimens is 196 kN), models were constructed such that the materials for both the model and the prototype were identical, thus following the concept of simple similarity, Tomazevic [6]. Structures dimensions and reinforcement layout are shown in Fig 1. The prototype followed nearly the configuration of a real building, but with slight modifications to fit the pattern of openings of doors and windows. Mechanical and physical properties of prototype and model materials are given in Table 1.

Walls were made of hand-made solid clay bricks confined by reinforced concrete TC´s and BB´s. In the direction of the earthquake simulator motion (E-W), three wall axes were built. The facade walls had door and window openings, whereas the middle walls were solid. In the prototype, the middle wall axis divides the two adjacent dwellings. In the transverse direction (N-S), four walls were built to improve the gravity load distribution among walls, and to control possible torsional deformations. Models were symmetrical and the wall distribution was uniform over the specimen height (i.e. M3).

TC´s and BB´s reinforcement was made of four longitudinal deformed wires and of hoops spaced at 100 mm. In M3, aimed at increasing wall shear strength, controlling damage and achieving a more stable behavior, hoop spacing was reduced to 30 mm at TC ends. Floor systems were cast-in-place reinforced concrete solid slabs supported on BB´s. Slabs were reinforced with 4,76 mm diameter deformed wires, spaced each 150 mm in both directions. The models were built on a steel platform.

To appropriately model the distribution of masses and live loads in the specimens, lead ingots were attached to the floor slabs. Lead ingots were oriented so that their impact on the slab flexural stiffness and strength was minimized. To correctly simulate the axial stresses on the walls of the prototype, additional prestressing forces were vertically applied onto the walls of the models and were kept constant throughout the testing program.

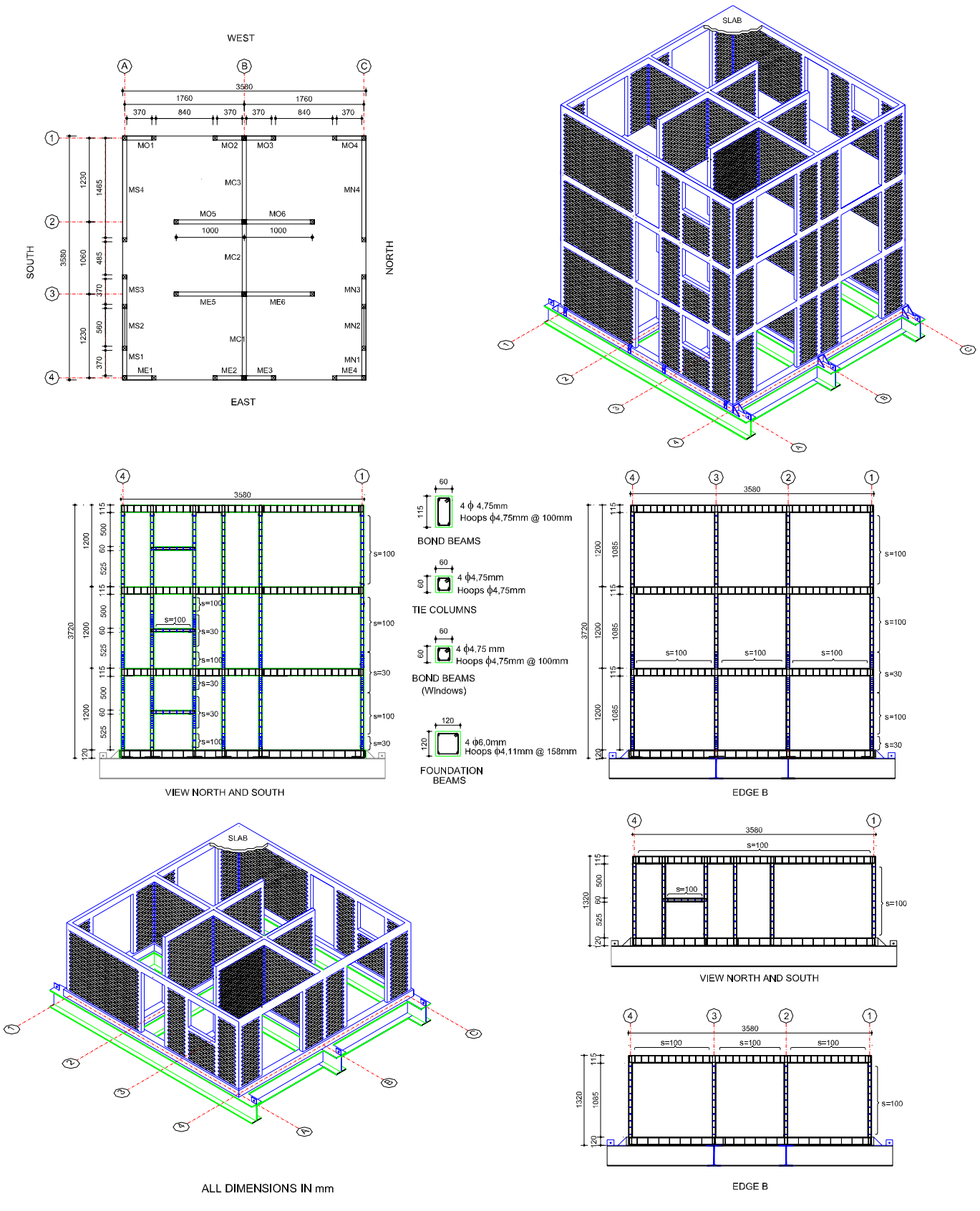


**Fig. 1 Characteristics of the Specimens**

**Table 1. Physical and Mechanical Characteristics of Prototype and Model**

| Property | Prototype | Model |
|---|---|---|
| Area in plan, $m^2$ | 51,28 | 12,82 |
| Size of door openings, mm | 970 x 2170 | 485 x 1085 |
| Size of window openings, mm | 1120 x 1000 | 560 x 500 |
| Story height, mm | 2400 | 1200 |
| Clay brick size, mm | 60 x 120 x 240 | 30 x 60 x 120 |
| Mortar joint thickness, mm | 10 | 5 |
| TC cross-sectional dimension, mm | 120 x 120 | 60 x 60 |
| BB cross-sectional dimension, mm | 230 x 120 | 115 x 60 |
| Slab thickness, mm | 120 | 60 |
| Size of foundation beams, mm | 240 x 240 | 120 x 120 |
| Diameter of longitudinal steel bars, in. (mm) | 3/8 (9,5) | 3/16" (4,76) |
| Hoop diameter, in. (mm) | ¼ (6,4) | 1/8 (3,2) |
| Maximum size of aggregate, in. (mm) | ¾ (19) | 3/8 (9,5) |
| Maximum size of sand grain, mm | 4,76 | 2,38 |
| Nominal strength of concrete, MPa | 19,6 | 19,6 |
| Nominal strength of mortar, MPa | 12,3 | 12,3 |
| Nominal yield stress of longitudinal steel, MPa | 412 | 412 |
| Nominal yield stress of hoops, MPa | 245 | 245 |

## Materials and Construction

Model clay bricks were especially manufactured in a typical brick factory near Mexico City. The mortar used to join the units had a cement:lime:sand ratio of 1:0,5:3,5 (by volume). The grading of the sand was scaled down to obtain a maximum size of 2,38 mm. The mortar joint had a thickness of 5 mm, with a 1-mm tolerance. In TC´s and BB´s, concrete with a cement:gravel:sand ratio of 1:2:3 (by weight), a maximum coarse aggregate size of 9,5 mm and a superplasticizer to facilitate concrete placement, were used. Deformed 4,76-mm diameter wires were used throughout for the longitudinal reinforcement of TC´s, BB´s and slabs; hoops were made of 3,2-mm diameter smooth wires. A heat-treatment process was required to adapt the wire stress-strain characteristics to those required by the rules of similarity, i.e. the characteristics of typical reinforcing steel in Mexico. In order to measure the mechanical characteristics of the materials, small-scale mortar cubes, concrete cylinders, masonry prisms, and square masonry walls, as well as wire coupons were sampled. Average measured mechanical properties of materials at the time of testing are shown in Table 2.

Both models were constructed following the regular practice in Mexico City. Walls were built by halves; firstly, the lower half of the walls, along with the lower half of the TC´s was constructed. Secondly, the upper half was built. Finally, BB´s and floor slabs were cast monolithically.

## Instrumentation and Test Program

To assess the global and local behavior, specimens were instrumented with acceleration, displacement and strain transducers. During the tests, story displacements, table and story accelerations, wall deformations and reinforcement strains were recorded.

Two earthquake motions recorded in epicentral regions in Mexico were used as basis for the testing program. One was the motion recorded in Acapulco, Guerrero, in April 25, 1989, during a M=6,8 earthquake with PGA=0,34g. The other was that recorded in Manzanillo, Colima, in October 10, 1995, during a M=8,0 quake with PGA=0,40g [7]. Both records were considered as Green functions to simulate larger magnitude events (i.e. with larger instrumental intensity and duration) [8]. For the Acapulco record, earthquakes with magnitudes 7.6, 7.8, 8.0 and 8.3 were simulated, whereas for the Manzanillo record,

earthquakes with magnitudes 8.1, 8.2 and 8.3 were simulated. Once the records were numerically calculated, acceleration and duration were scaled, both in acceleration and duration, to fulfill the requirements of similarity models.

**Table 2. Mechanical Properties of Materials (MPa)**

| | M1 | M3 |
|---|---|---|
| Compressive strength of clay brick units | 11,8 | 11,8 |
| Compressive strength of mortar (cubes) | 19,7 | 16,2 |
| Compressive strength of masonry (prisms) | 7,0 | 6,9 |
| Axial stiffness of masonry (prisms) | 1630 | 1974 |
| Diagonal compression strength of masonry (walls) | 1,20 | 1,18 |
| Shear modulus of masonry (walls) | 1250 | 807 |
| Compressive strength of concrete (cylinders) | 26,2 | 21,8 |
| Elastic modulus of concrete | 17801 | 17009 |
| Yield stress of longitudinal reinforcement | 493 | 493 |
| Strength (ultimate stress) of longitudinal reinforcement | 584 | 584 |
| Yield stress of hoop reinforcement | 269 | 269 |
| Strength (ultimate stress) of hoop reinforcement | 320 | 320 |

M1 and M3 were subjected to a sequence of seismic excitations by gradually increasing the intensity of motion at each test run up until the final damage state was attained. Because during testing of the specimens, expected performance levels (i.e. damage states) were not attained due to the large lateral strength and stiffness of the specimens, several modifications were done to the models. In M1, walls MC1 and MC3 were fully eliminated (Fig. 1), walls ME5, MO5, ME6, MO6 were cut into small narrow walls, and a 47 percent extra mass was added. In M3, only walls MC1 and MC3 were eliminated. A total of 28 and 13 test runs were applied to M1 and M3, respectively. Between each test run, a random acceleration signal (white noise) at 50 cm/s$^2$ (0,05 g) RMS was applied to identify changes in the dynamic properties.

## TEST RESULTS

### Crack Patterns

Final patterns of cracking are shown in Fig 2. As it was mentioned, models with their original wall configuration only suffered minor cracking suggesting behavior within the elastic range. At this stage, the response was characterized by horizontal cracks at the base of the walls. After removing the wall above mentioned, and at larger intensity motions, damage in both specimens was governed by inclined cracking of the N and S facades. Simultaneously, horizontal cracks uniformly distributed over the TC´s and walls on the E and W sides were observed. Slabs also showed cracking perpendicular to the direction of the base motion attributed to slab bending at the door openings. At the end of the tests, damage was characterized by crushing of the masonry walls, cracking and crushing of the concrete TC´s and by kinking of the longitudinal steel at the TC´s ends (dowel action). Similarly, shallow cracks in walls MO1 and MO4 at the West side, and out-of-plane sliding in walls MS4 and MN4 was observed, which suggests some torsional response. Analysis of data later confirmed that shear deformations controlled the response.

In M1, damage was mainly characterized by horizontal and inclined cracks. The first inclined cracks formed near the wall center, and propagated towards the corners TC´s ends, except for walls MS4 and

MN4, where behavior was dominated by a shear-sliding mechanism (horizontal cracks at the walls base) and inclined cracks in the lower part. First diagonal cracking occurred at a drift ratio to 0,36%. Crack propagation into the TC´s ends, thus shearing off these elements, was recorded at a drift ratio to 0,67%. At the end of the test runs, maximum recorded drift ratio was 1,83%.

In M3, damage was mainly concentrated in the first story (ground floor). In general, walls exhibited one or two large inclined cracks at 45-deg (X-shaped). First diagonal cracks formed at a drift ratio to 0,25%. Penetration of inclined cracking to TC´s ends was recorded at a drift ratio to 0,43%. A full soft-story mechanism was readily observed during test runs for which the maximum recorded drift ratio was 1,75%. In the second story, few horizontal cracks at the base of the walls were observed, whereas in the third story no cracking was observed.

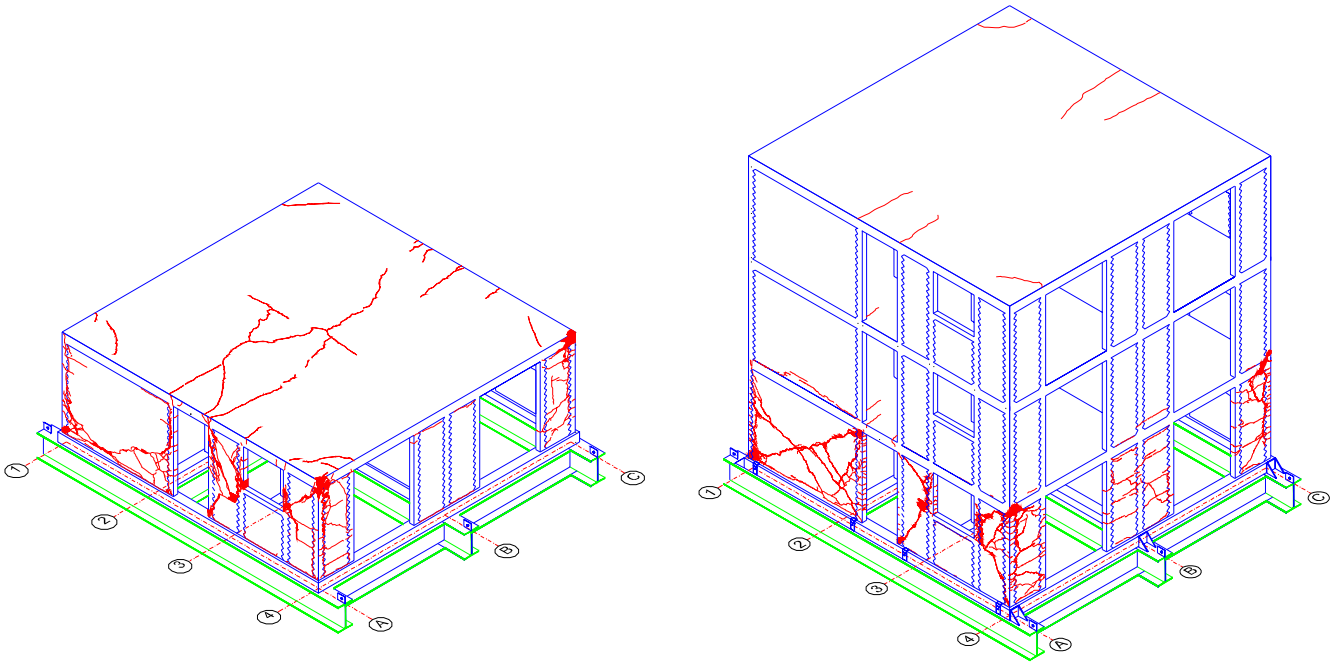

**Fig. 2 Final Cracks Patterns**

**Hysteresis Curves**

To assess the overall performance of structures M1 and M3, the hysteresis curves in terms of the base shear and lateral drift ratio of the first story are shown in Figs. 3 and 4, respectively. The base shear was calculated from measured accelerations at each floor slab center of gravity and by considering the specimen mass and extra mass from lead ingots.

Hysteresis loops were typical of CM structures. To facilitate comparison between specimens, and among other specimens tested under dynamic or static conditions, three limit states were defined: elastic (E), maximum or strength (M) and ultimate (U).

The elastic limit was defined by the occurrence of the first inclined cracking in the masonry wall; strength was achieved when the maximum base shear was resisted; and the ultimate limit state was considered at a lateral drift ratio when 20 percent reduction in strength was recorded. Cycles within the elastic limit

experienced some hysteresis attributed to wall flexural cracking at initial stages. As it is common in CM structures, specimens attained their strength at loads higher than those associated to first inclined cracking. Specimen M1 showed stable and symmetric loops up to large drift ratios, whereas in M3, hysteresis curves were stable and symmetric up to the strength limit state, after which a severe strength and stiffness decay, because of damage over the panels and at TC´s ends, was developed. As it is customary in shear-governed members subjected to inelastic deformations, response curves exhibited severe pinching, especially at very large lateral drift ratios associated to failure of the structure. In M3, at the ultimate limit state, a fast degrading process, involving sliding along the first story inclined cracking and crushing of masonry and concrete, was clearly observed. It was apparent that stories 2 and 3 laterally deformed very slightly, suggesting a rigid body motion over the first story. This phenomenon led to a concentration of deformations and damage at the first story which performed as a soft-story with a shear-governed mechanism.

The envelope curve for M3 in Fig. 4 is drawn with different colors and markers depending on the specimen wall layout. The line and square markers in blue correspond to the specimen with the original wall layout. For this structure, the wall density index was 4,1 percent. The wall density index was calculated as the ratio of the wall area in the direction of loading and the floor plan area. The line and round markers in red relate to the specimen response after MC1 and MC3 had been removed (walls removed are indicated by two red X's in the figure), thus leading to a lower wall density index (2,9 percent). Wall removal in the middle axis evidently modified the trend of the envelope curve. In an effort to visualize a possible envelope should the original wall index had been kept constant, envelope values for the modified specimen (i.e. without walls MC1 and MC3) were affected by the ratio of the wall density indexes, namely, 4,1 / 2,9=1,4. The envelope of this virtual specimen is shown with the line and triangles in green.

Comparing the shape of the envelope curves for M1 and M3, as well as the force and drift ratio values for the three limit states identified, it is apparent the similitude in the response. The latter supports the idea that the performance of the three-story structure, M3, was controlled by the first story which, in turn, was governed, as in M1, by shear deformations.

Also drawn in the response envelopes curves in Figs. 3 and 4 are the strength predictions using the Mexico City Building Code requirements, MCBC [9-10]. The calculation involved measured material properties at testing and actual wall dimensions. It is clearly evident that the specimens´ overstrength were 2,0 and 1,3, for M1 and M3, respectively.

Test results are summarized in Table 3. Seismic shear coefficients and first story drift ratios at the limit states selected are presented for M1 and M3. For comparison, the results two-story full-scale 3D structures tested under static lateral loading are also included [11]. It is apparent that for M1 and M3, drift ratios at first inclined cracking (i.e. limit of the elastic range) were more than double the average drift observed in static tests. On the other hand, drifts at strength in dynamic and static tests were comparable for M3, but much larger for M1. These findings are quite important because, many design regulations, such as Reference 10, limit the lateral drift ratios to values that were basically derived from static tests on isolated walls and wall subassemblages. For example, the inclined cracking lateral drift ratio for design is 0.15%, whereas the inelastic drift ratio permitted for CM structures is 0.25%. From these results it is clear that drift ratios for inclined cracking could be increased, while the largest drift to be permitted should be limited to that observed at strength, i.e. 0.4%, approximately. Evidently more studies and data are needed, especially to consider the variability of drift ratios.

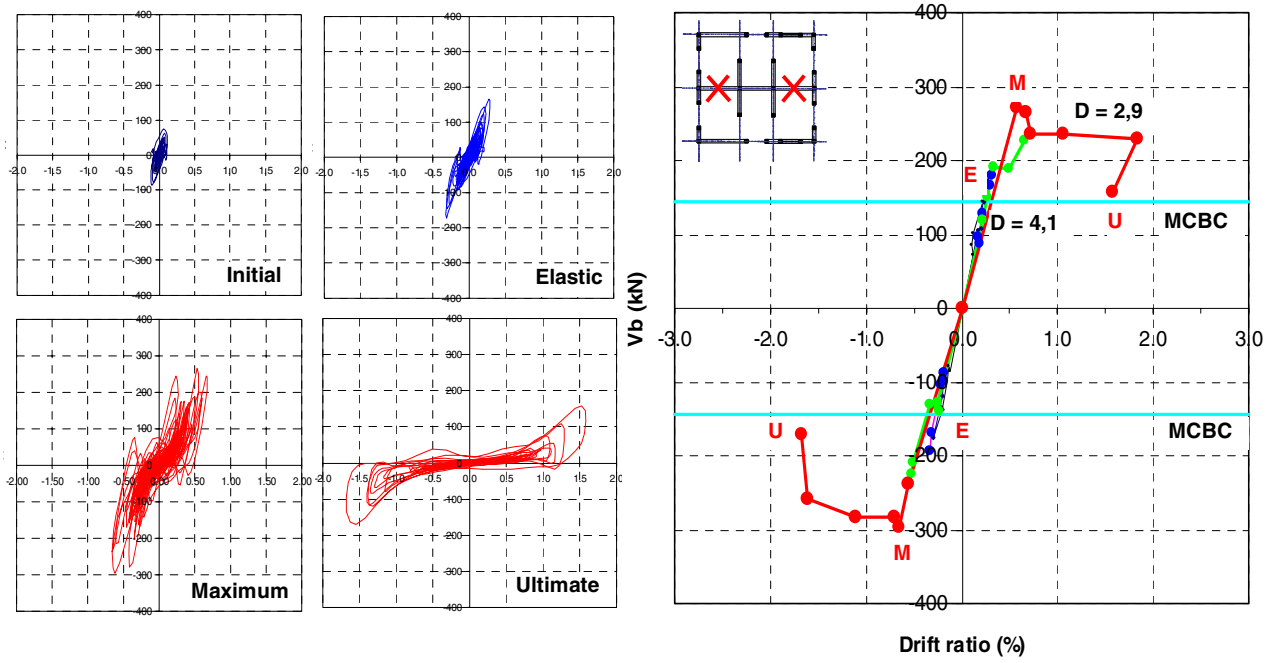


**Fig. 3 Hysteretic Curves and Response Envelope for M1**

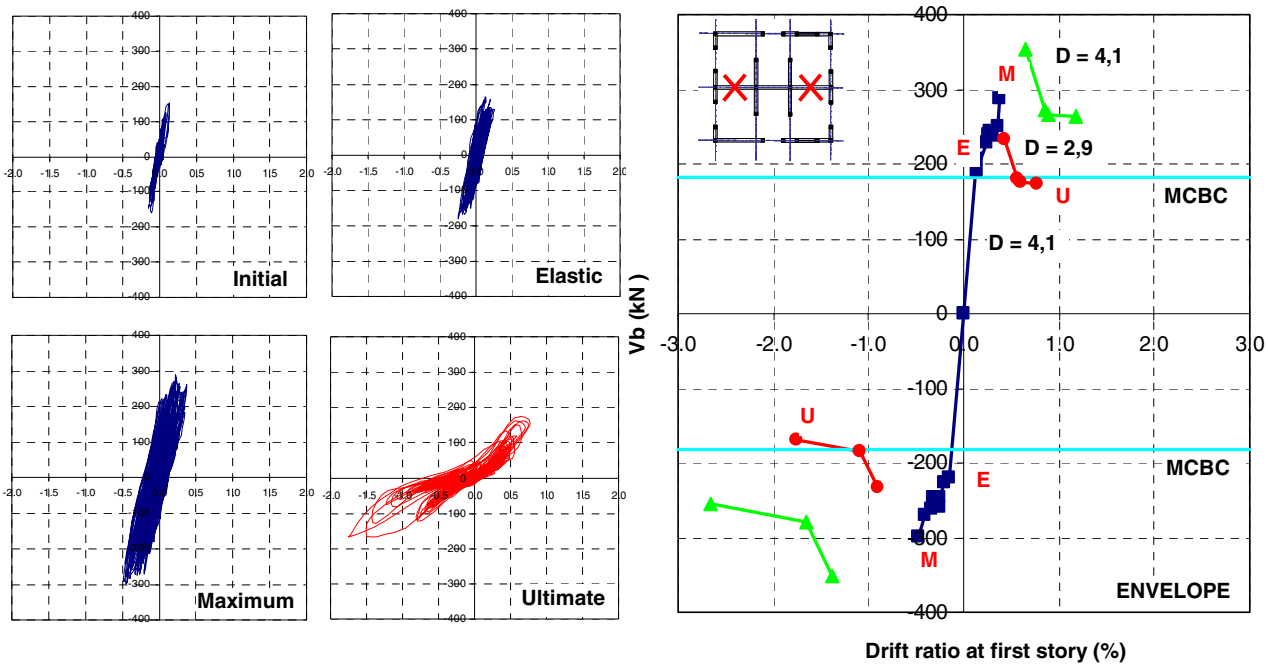


**Fig. 4 Hysteretic Curves and Response Envelope for M3**

**Table 3. Measured response characteristics**

| Test | Model | Seismic shear coefficients (g) | | | | Drift ratio at first story (%) | | | |
|---|---|---|---|---|---|---|---|---|---|
| | | Elastic | Maximum | Ultimate | Maximum / Elastic | Elastic | Maximum | Ultimate | Maximum / Elastic |
| Dynamic | M1 | -3,83<br>3,56 | -4,18<br>3,74 | -2,41<br>2,22 | 1,09<br>1,05 | -0,36<br>0,28 | -0,66<br>0,67 | -1,61<br>1,83 | 1,83<br>2,39 |
| | M3 | -1,53<br>1,44 | -1,71<br>1,58 | -1,27<br>1,31 | 1,12<br>1,10 | -0,26<br>0,24 | -0,48<br>0,38 | -1,75<br>0,79 | 1,85<br>1,58 |
| | | | | | | | | | |
| Static | 3D | -2,56<br>2,80 | -3,17<br>3,43 | -2,69<br>2,63 | 1,24<br>1,23 | -0,08<br>0,13 | -0,39<br>0,36 | -0,55<br>0,50 | 4,88<br>2,77 |

To assess the force response of M3 under dynamic excitations, envelopes of the maximum lateral forces induced by the runs were plotted for the limit states above mentioned (Fig. 5). The inertial force at each floor slab was calculated by multiplying the maximum recorded acceleration in the slab center of gravity and the tributary mass of that particular story. The tributary mass comprised the masses of the slab and lead ingots, plus half of the mass of walls above and/or below the story.

From the graph is evident that lateral force distributions up to the elastic limit clearly followed the commonly assumed triangular shape distribution. This is an indication that the first mode was the fundamental mode of vibration. In contrast, for larger lateral drift ratios, when the maximum load carrying capacity (strength) and ultimate were reached, force distributions changed by concentrating the forces in the first story, again suggesting the formation of a soft-story mechanism (see the cyan line for the ultimate limit state).

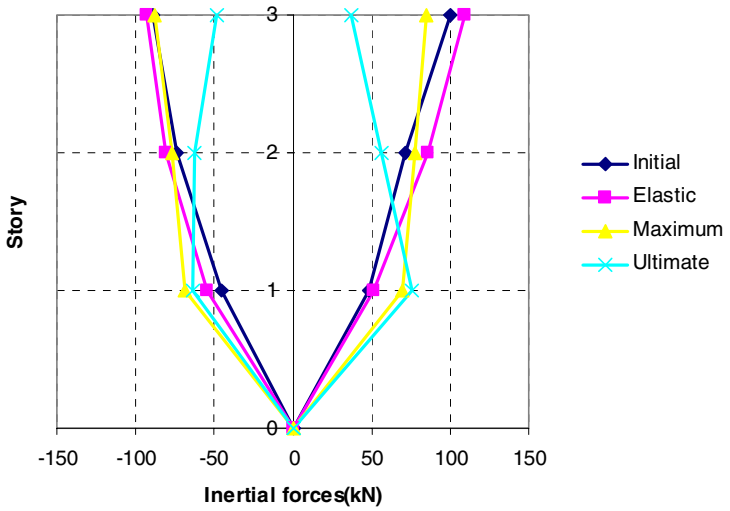


**Fig. 5 Lateral Force Distribution for Different Limit States for M3**

**Stiffness Degradation**

Previous test programs aimed at assessing the main characteristics of the hysteretic response of CM structures have indicated that loss of stiffness is typical even at drift ratios significantly smaller than those at initial inclined masonry cracking. Moreover, a parabolic decay has been noted so that at drift ratios to 0.5%, the remaining stiffness is of the order of 20 percent of the initial, uncracked stiffness [4]. To assess

the stiffness degradation phenomenon, peak-to-peak stiffnesses, $K_p$ were calculated for representative cycles in both models. Normalized peak-to-peak stiffness - first story drift ratio curves for M1 and M3 models are shown in Fig 6. The peak-to-peak stiffnesses were normalized with respect to the initial stiffness of M1 and M3. Similarly to the envelope curves for M3, values corresponding to the specimens with modifications in the wall layout are presented with different colors in lines and markers.

Stiffness decay was observed at low drift ratios, even before first inclined cracking became apparent. This phenomenon is attributed to incipient wall flexural cracking, and perhaps, to some micro-cracking (invisible to the naked eye) in masonry materials, local loss of mortar bond and adjustment of brick position. After first inclined cracking, but before reaching strength, the decay increased with drift ratio. At larger drift ratios, $K_p$ remained nearly constant. At this stage, stiffness decay is associated to cracking and crushing in masonry walls and RC confinement members.

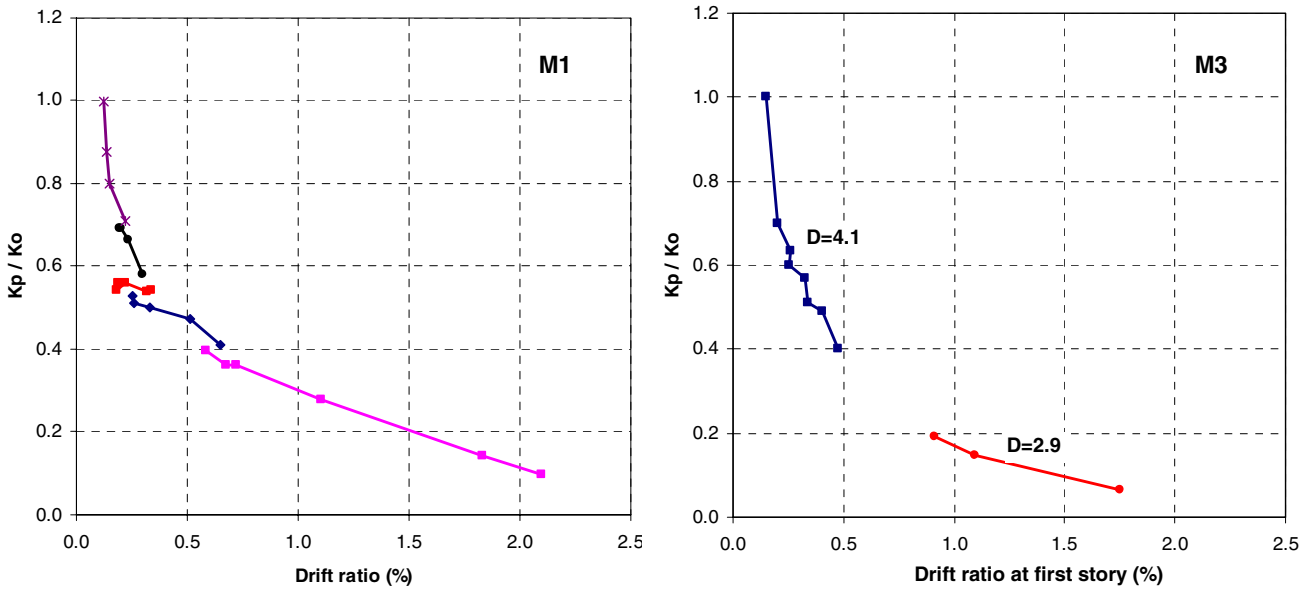


**Fig. 6 Stiffness Degradation**

The response recorded for M1 and M3 closely resembles that calculated for specimens tested under static loading in Mexico, as can be noted by comparing to several stiffness curves included in Fig. 7. Such figure is taken from Flores [3].

**Energy Dissipation**

The energy dissipated during the tests was computed as the area within the hysteresis loops from the base shear–drift relations. The total cumulative energy dissipated for M1 and M3 are shown in Fig.8. It is evident that M1 dissipated, in absolute terms, more energy that M3; moreover, at same drift ratios, M1 also dissipated more energy. At present, it is contended that the failure mode of M1, characterize by shear and sliding mechanisms, contributed to the difference.

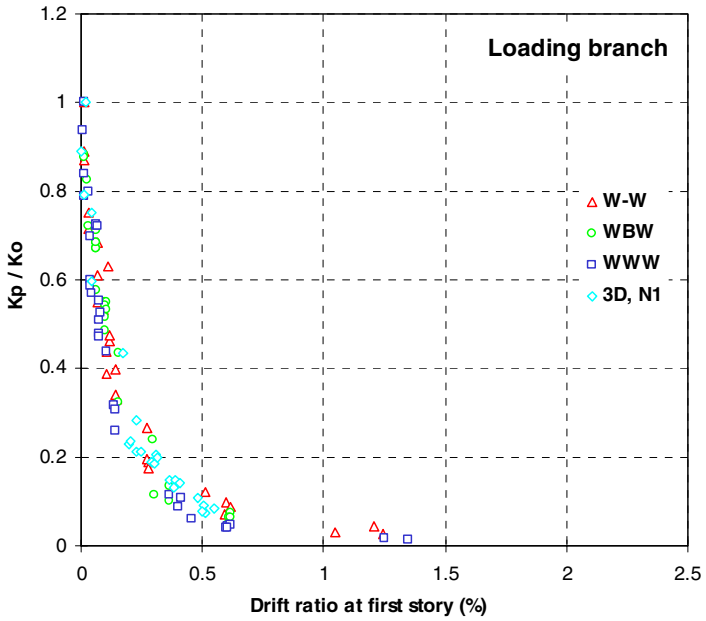


**Fig. 7 Stiffness Degradation from Statically Tested Specimens**

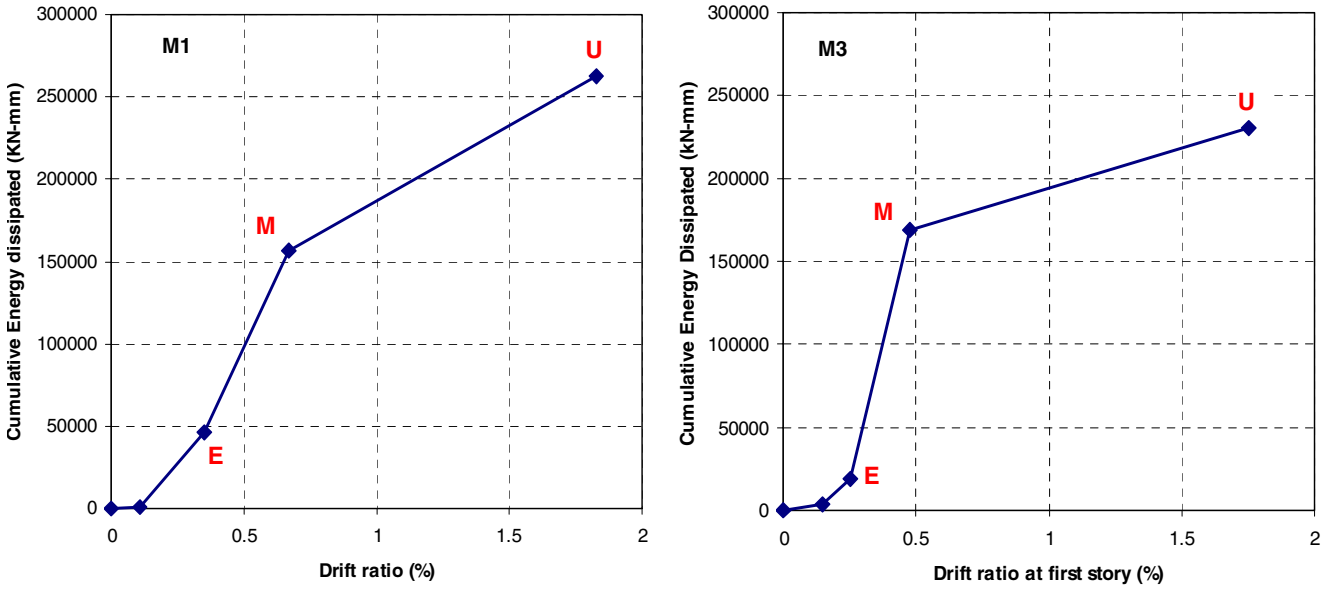


**Fig. 8 Energy Dissipated**

## CONCLUSIONS

Based on the observations made during the tests and the limited data analysis conducted so far, it may be concluded that the dynamic performance of CM structures clearly indicated that actual design requirements in Mexico are quite safe; actually, are quite conservative. This conclusion may justify the need for reducing the number and complexity of stringent requirements in the code. Comparing the calculated and the measured strengths, it was found that the level of overstrength of CM structures is of the order of 2. Also it was found that the drift ratio corresponding to cracking was about 2,5 times the average value observed in static tests, and that the maximum drift ratio to be allowed for the design of CM structures is 0.4%. Such results are of significance should a performance based seismic design approach is decided for CM structures. Based on the failure mode observed, the analytical model for design and assessment could be simplified by assuming that all inelastic deformations would take place at the first story and would be controlled by shear.

## ACKNOWLEDGMENTS

The research program was financially supported by the Consejo Nacional de Ciencia y Tecnología (CONACYT-Mexico). The help of the staff of the Shaking Table Laboratory at the Institute of Engineering of the National University of Mexico is thankfully acknowledged.

## REFERENCES

1. Ishibashi K, Meli R, Alcocer S M, León F, and Sánchez T. "Experimental study on earthquake resistant design of confined masonry structures." Proceedings of the 10th World Conference on Earthquake Engineering, Madrid, Spain. Rotterdam: Balkema, 1992; 6: 3469-3474.
2. Alcocer S M, Meli R. "Test program on the seismic behavior of Confined Masonry Structures." The Masonry Society Journal 1995; 13(2): 68-76.
3. Flores L E, Alcocer S M, "Calculated response of confined masonry structures." Proceeding of the 11th World Conference on Earthquake Engineering, Acapulco, Mexico. Paper no. 1830. Oxford: Pergamon, 1996.
4. Zepeda J A, Alcocer S M, and Flores L E. "Earthquake-resistant construction with multi-perforated clay brick walls." Proceedings of the 12th World Conference on Earthquake Engineering, Auckland, New Zealand. Paper no. 1541. Elsevier science, 2000.
5. Alvarez J J, Alcocer S M, and Contreras J. "Nonlinear analytical behavior of walls with openings subjected to lateral loads." Proceedings of the 2nd Ibero American Congress on Earthquake Engineering. Madrid, Spain. Paper no. 016.1: 2001.
6. Tomazevic M, Velechovsky T. "Some aspects of testing small-scale masonry building model on simple earthquake simulator." Earthquake Engineering and Structural Dynamics 1992; 21: 945-63.
7. Sociedad Mexicana de Ingeniería Sísmica. "Base Mexicana de Datos de Sismos Fuertes." Mexico, 1997.
8. Ordaz M, Arboleda J. "Instructivo para los programas Simfi2 y Genbet3." National Center for Disaster Prevention, CENAPRED, Mexico 1993.
9 Alcocer S M, Cesín J, Flores L E, Hernández O, Meli R, Tena A, and Vasconcelos D. "The new Mexico City Code Requirements for Design and Construction of Masonry Structures," Proceeding of the 9th North American Masonry Conference. South Caroline, USA. Paper no. 4B.3: 2003.
10. Mexico City Building Code. Gaceta Oficial. Gobierno del Distrito Federal. 2004.

11. Sánchez, T.“Estudio Experimental sobre una Estructura de Mampostería Confinada Tridimensional, Construida a Escala Natural y Sujeta a Cargas Laterales” Proceedings of the 10th National Congress on Structural Engineering. Mérida-Yucatán, Mexico, 1996;II: 909-918.